# Calorimeter Physics (general and aspects of LHC experiments)

Claudio Santoni UBP IN2P3/CNRS
Clermont-Ferrand France

# Outline

- Calorimetric measurements
  - Electromagnetic calorimeters
  - Hadronic calorimeters
- From Photons to GeV (Calibration of TileCal Cells)
- From Particles to Jets (Measurement of Jets in ATLAS)

# Showers Development

- Neutral and charged particles incident on a block of material deposit their energy through creation and destruction processes
- The deposited energy is rendered measurable by ionization or excitation of the atoms of matter in the active medium
- The active medium can be the block itself (homogenous calorimeter) or light active layers sandwiched with dense absorber layers (sampling calorimeter)

The development of EM showers $(e, \gamma)$ is characterized by

- the Critical Energy

$$\varepsilon \cong \frac{560}{Z}\ [\mathrm{MeV}]$$

above which radiation overcome ionization (in the case of lead $\varepsilon \cong 7\ [\mathrm{MeV}]$) and

- the Radiation Length defined by the distance over which the electron loses, on average, all but 1/e of its energy

$$X_0 = \frac{180A}{Z^{1/3}}\ [\mathrm{gcm}^{-2}]$$

(in the case of lead $X_0 = 0.56\ [\mathrm{cm}]$)

The development of hadronic showers $(\pi, p, ..)$ is characterized by

- the Interaction Length

$$\lambda = 35 \times A^{1/3} [\mathrm{gcm}^{-2}]$$

In the case of materials used in calorimetry $\lambda$ ranges between 10 and 40 cm

# Electromagnetic Cascade

## Longitudinal Development

- Critical energy electrons do not travel far ($\cong 1\ X_0$). After the shower maximum, the remaining energy of the cascade is carried forward by $\gamma$'s giving the typical exponential falloff
- The different shapes are due to lower $\epsilon$ for higher Z material

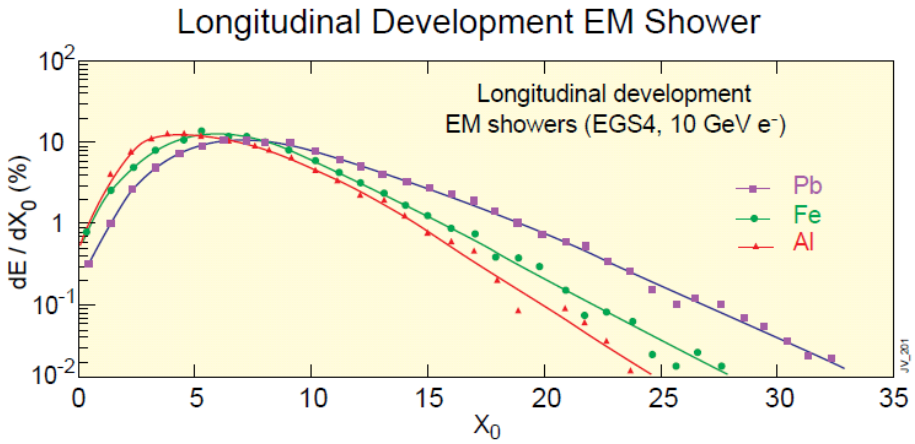


## Lateral Development

- The e.m. shower begins, and persists, with a narrow core of high energy cascade particles, surrounded by a halo of soft particles which scatter increasingly as the shower depth increases
- In different material the lateral extend scales with the Moliere radius

$$R_M = \frac{7A}{Z}\,[\mathrm{gcm}^{-2}]$$

- An infinite cylinder with a radius of 1 $R_M$ contains about 90% of the shower energy

# Hadronic Cascade

## Longitudinal Development

- The interaction responsible for shower development is the strong interaction rather than electromagnetic
- The cascade contains two distinct components namely the electromagnetic one ($\pi^0$) and the hadronic one ($\pi^{\pm}$, n)
- The number of independent particles in the hadronic cascade is smaller by $E_{th}/\varepsilon$. The intrinsic resolution will be worse at a least by a factor $\sqrt{(E_{th}/\varepsilon)} \cong 3$ ($E_{th} \cong 2m_{\pi} = 280$ MeV)
- Over 9 interaction lengths ($\lambda$) are required to contain almost all the energy of high energy hadrons

## Lateral Development

- High energy hadronic showers show a pronounced core, caused by the $\pi^0$ component with a characteristic transverse scale of $R_M$, surrounded by an exponentially decreasing halo with scale $\lambda$.

# Energy Response and Resolution

- The energy response of calorimeters is parameterized as

$$E_{vis} = LE + N$$

  - Where $E_{vis}$ is the visible energy, $L$ is the linearity term and $N$ includes the energy equivalent to the electronics noise and the energy carried by particles other than the one(s) of interest (pileup)

- The energy resolution is parameterized as

$$\frac{\sigma}{E} = \frac{\sigma_{stoc}}{E} \oplus \frac{\sigma_{noise}}{E} \oplus \frac{\sigma_{lin}}{E} = \frac{a}{\sqrt{E}} \oplus \frac{b}{E} \oplus c$$

  - The first term, with coefficient $a$, is the stochastic term and accounts for statistical fluctuations in the number of signal generation processes
  - The second term, with coefficient b, is the noise term and includes the fluctuations in $N$
  - The last term, with coefficient c, is the constant term that accounts for the fluctuations in $L$ due non uniformities, the amount of energy leakage and the contribution from e.m component in the hadronic shower

# Energy Resolution of EM Homogenous Calorimeters

- In homogenous calorimeters the stochastic term is determined by the fluctuation in the number *n* of ions and/or photons produced. If *W* is the mean energy required to produce an electron-ion pair (or a photon) then $n = E/W$, and

$$\frac{\sigma_{stoc}}{E} = \frac{\sigma_i}{E} = \frac{\sqrt{n}}{n} = \frac{\sqrt{W}}{\sqrt{E}} \rightarrow a = \sqrt{W}$$

- Lead glass shower detectors are based on the detection of the Cerenkov light, produced by electrons and positrons with kinetic energy larger than $\cong 0.7$ MeV. This means that at most $1000/0.7 \cong 1400$ independent particles, per GeV of deposited energy, produce Cerenkov light. The resolution is then dominated by the fluctuation in this number and is $\geq\ 3\%/\sqrt{E[GeV]}$ . This is further limited by photo-electron statistic as only about 1000 photo-electrons are generated when using photomultipliers to detect the scintillation light.

# Energy Resolution of Sampling EM Calorimeters

- When the very best energy resolution is not required, sampling calorimeters are employed
- The shower energy is measured in active layers, often of low $Z$, sandwiched in between passive absorber layers of high $Z$ material.
- The energy resolution is dominated by the fluctuations of the shower energy dissipated in the active medium ($\sigma_s$)
- If the energy loss in an active layer is much smaller than that in the absorber layer the number of independent charged particles crossing an active layer can be approximated by $n = E/\Delta E_{abs}$ where $\Delta E_{abs}$is the energy lost by a minimum ionizing particle (m. i. p.) in the absorber layer. Now $\Delta E_{abs} = t_{abs} \times (dE/dx)$. Hence

$$\frac{\sigma_{stoc}}{E} = \frac{\sigma_s}{E} = \frac{\sqrt{n}}{n} \approx \frac{\sqrt{t_{abs}}}{\sqrt{E}}$$

- An empirical valid formula is

$$\frac{\sigma_s}{E} \cong \frac{4\%\sqrt{\Delta_{cell}[MeV]}}{\sqrt{E[GeV]}}$$

where $\Delta_{cell}$ is the m. i. p. energy loss in sampling cell (absorber plus active medium)

# Energy Response of Hadronic Calorimeters

- Hadronic calorimeters, because of the large depth required ($\cong 10\ \lambda$) are by necessity sampling calorimeters. The response of the calorimeter to electrons can be expressed as

$$E_{vis}^{e} = eE$$

$$E_{vis}^{\pi} = eE_{em} + \mathrm{c}E_{ch} + nE_n + NE_N = eE_{em} + hE_{had} = [eF_0 + h(1 - F_0)]E$$

where $E, E_{vis}^{e}$ and $E_{vis}^{\pi}$ are incident and visible energies respectively. $E_{em}, E_{ch}$ and $E_N$ the energy deposited by electromagnetic component and charged hadrons (low energy neutrons and energy lost in breaking up nuclei). Each component has its own sampling fraction.

- The sampling fraction $N$ is normally very small and $E_N$ can be large. Hence $e/h$ is in general larger than 1.

- $F_0$ is the e.m. component of hadronic shower. In iron $F_0$ increase from 50% to 70% when the energy of the incident pions ranges between 10 and 50 GeV -> response in energy to hadrons not linear

# Energy Response of Hadronic Calorimeters (cont)

- The degree of compensation is expressed by the energy independent ratio $e/h$
- It can not be measured directly but can be inferred from the energy dependent $E^e_{vis}/E^\pi_{vis} = e/\pi$ signal ratios

$$\frac{e}{\pi} = \frac{e/h}{1 + (e/h - 1)F_0}$$

$F_0 = 1 - (E[GeV]/0.76)^{-0.13}$ D. Groom

or

$F_0 = 0.11 \ln E\ [GeV]$ R. Wigmans

**TileCal result**

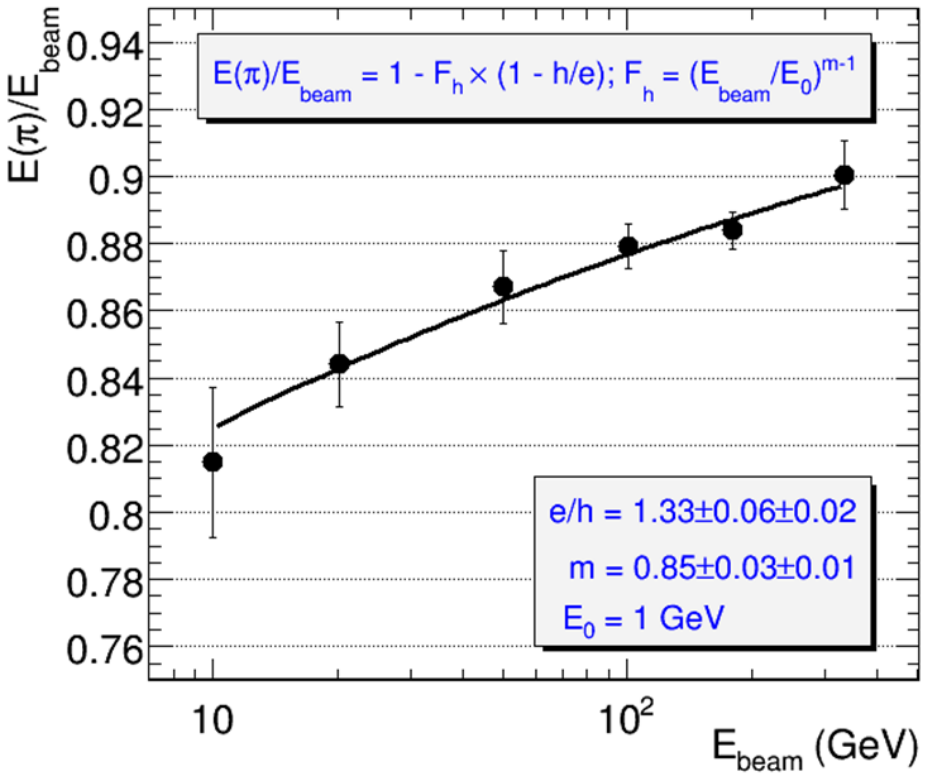

# Energy Resolution of Hadronic Calorimeters

- The stochastic term is given by

$$\frac{\sigma_{stoc}}{E} = \frac{\sigma_s}{E} \oplus \frac{\sigma_i}{E_i} = \frac{10\%\sqrt{\Delta E_{cell}}}{\sqrt{E}} \oplus \frac{\sigma_{comp}}{E}$$

- The sampling fluctuations for hadrons are larger than those for e.m showers by a factor of ≅3
- The intrinsic resolution $(dE/E)_{Comp}$ depends on $e/h$ and vanishes for a compensating calorimeter.
- The event-to-event fluctuation in $F_0$ affect the energy resolution. The average number of $\pi^0$ 's in a shower is small and its fluctuations large. This number increases as $\ln E\ [GeV]$ and

$$\frac{\sigma_{comp}}{E} \approx \frac{1}{\ln E\ [GeV]}$$

**Pion Energy Resolution of a copper quartz fibre Calorimeters**

Charged particles traversing the fibres generate Cerenkov light predominantly from the electromagnetic component (charged hadrons have a very high Cerenkov threshold).

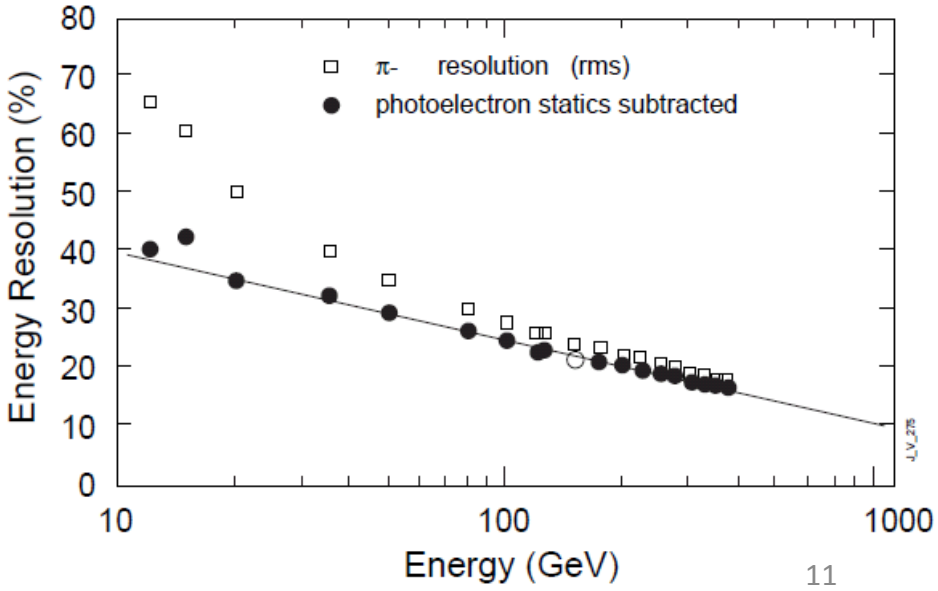

# A compensation weighting method (CDHS)

To suppress e.m. response a simple algorithm reduces the response of individual counters $i$ of the calorimeter by a fraction proportional to the un-weighted response $(E_i)$:

$$E'_i = E_i(1 - C'E_i)$$

- The optimum value for $C'$depends on the incoming pion energy, $C'$ was then parameterized as a function of the total un-weighted energy $E$ to make this procedure useful when the hadron energy is not known a priori

$$C' = C/\sqrt{E}$$

- The resolution per hadronic showers improves by 30% at 140 GeV and by 10% at 10 GeV

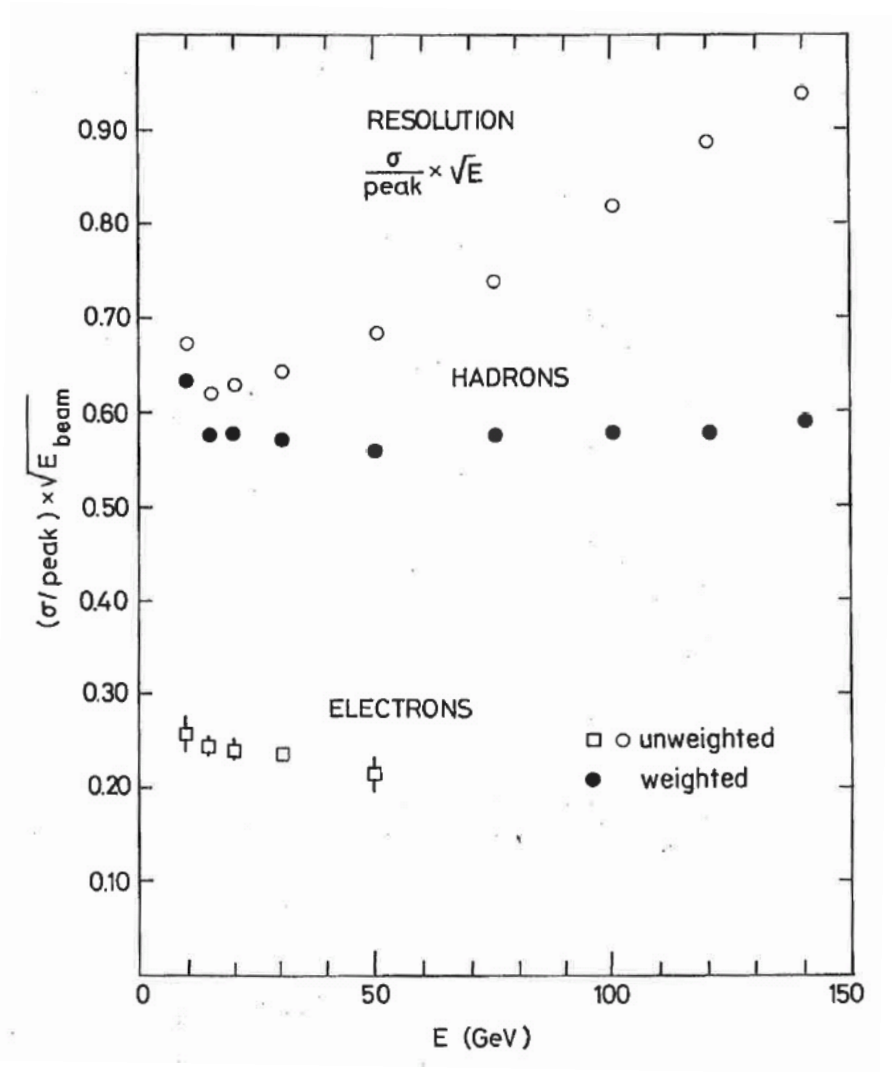

# The ATLAS Calorimeters

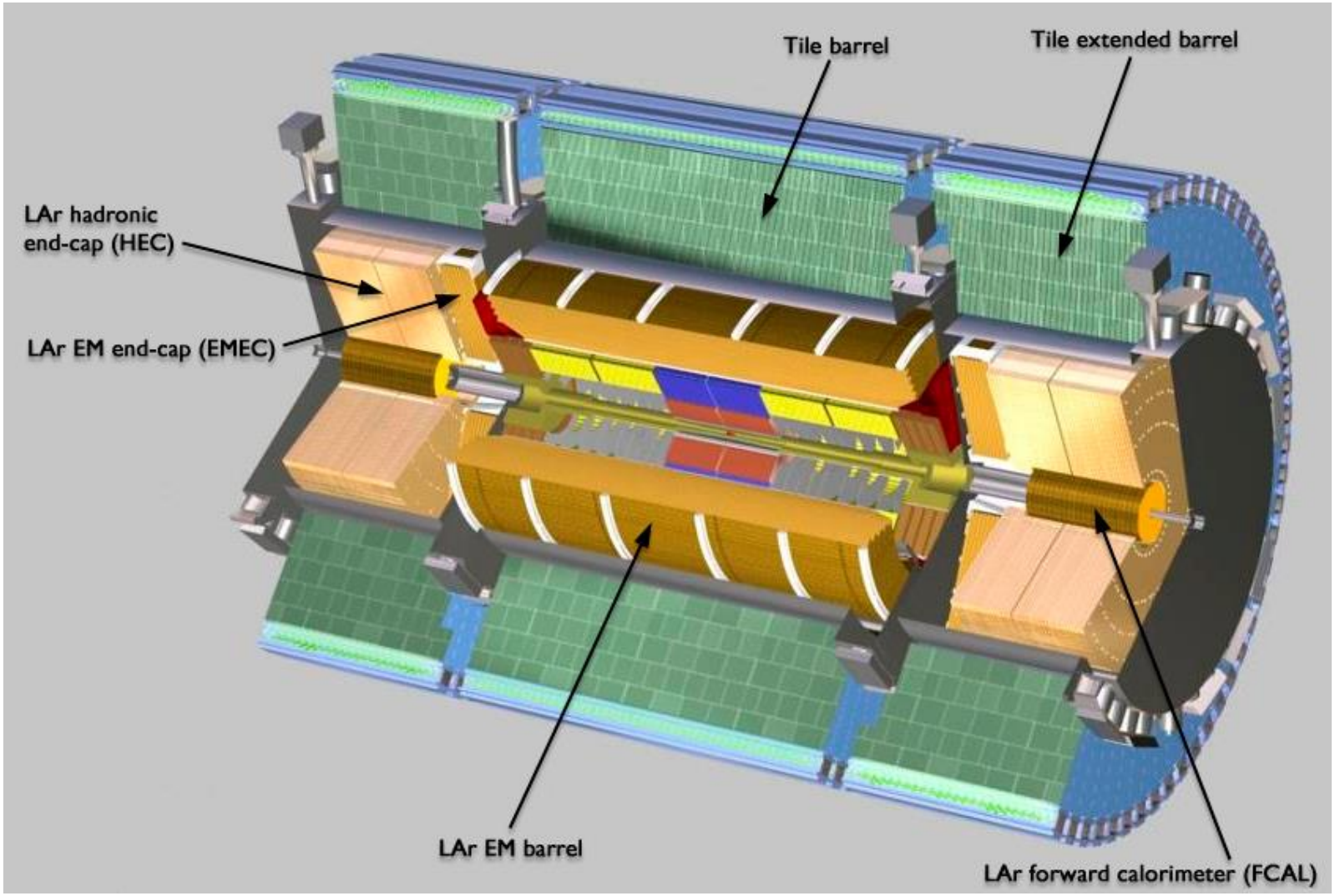

# The ATLAS TileCal Calorimeter

- 3 cylinder of 64 modules each spanning the azimuth angle $\Delta\phi=2\pi/64\cong0.1$.
- Depth: 7.4 $\lambda$
- The steel plates (4-5 mm) and scintillating tiles (3 mm) are perpendicular to the beam -> $\sqrt{\Delta E_{cell}} \cong 4$ MeV and $\sigma_s \cong 40\%$ at $\eta = 0.35$
- It is not a compensating calorimeter:

$$e/h = 1.33 \pm 0.07$$

- Energy resolution:

$$\frac{\sigma}{E} = \frac{(52.9\pm0.9)\%}{\sqrt{E}} \oplus (5.7 \pm 0.2)\%$$

  - The noise term is negligible
  - The constant term is affected by longitudinal containment

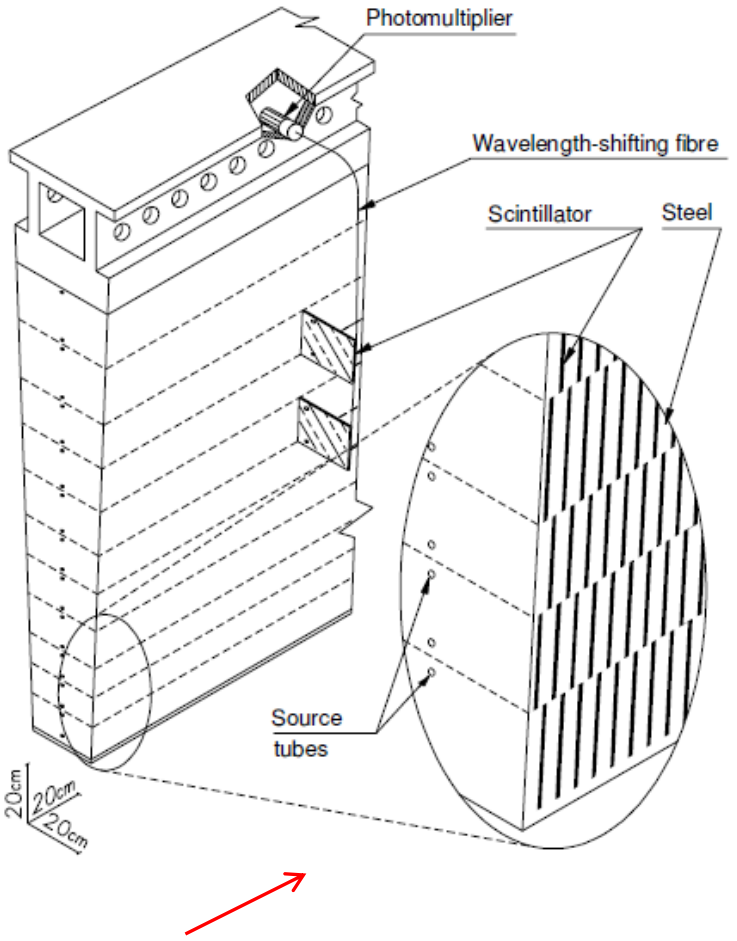

# The Monitoring Systems

The shower energy is obtained as the sum of the energy measured in each PMTs. Non uniformities and instabilities affect the detemination

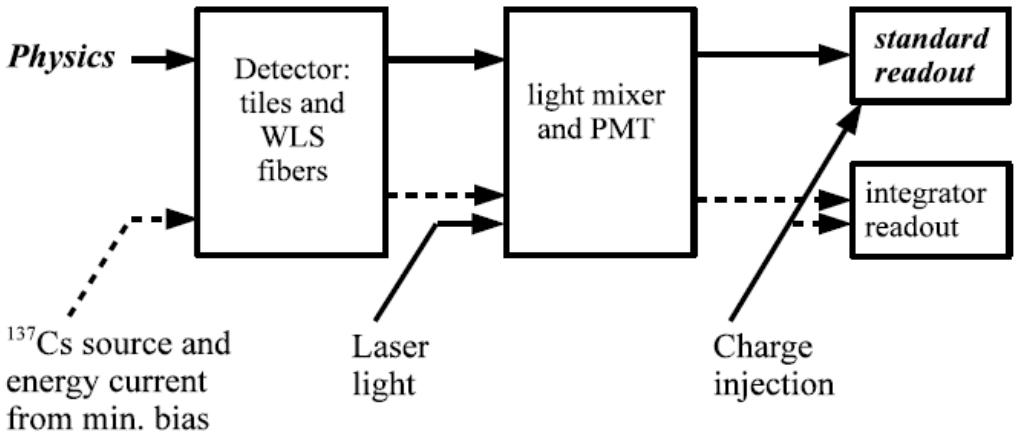


- Monitor gain stability by injecting laser light (532 nm) in each of 9836 PMT's (precision: <1%)
  - The PMTs need to operate in a stable way. A change of 1 V in the operating voltage gives a 1% variation in gain

# The Monitoring Systems

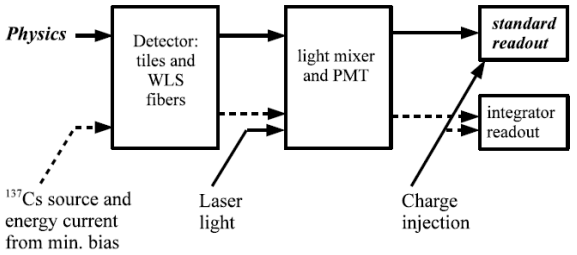


- Cs source (precision: 0.3%)
  - PMT voltage adjustments to inter calibrate cells response

  The range of the 0.662 MeV $\gamma$'s emitted by the $Cs$ source is very limited ($\cong$ 1 cm). The equalization of the cell response is achieved using a Sr source scan and muons

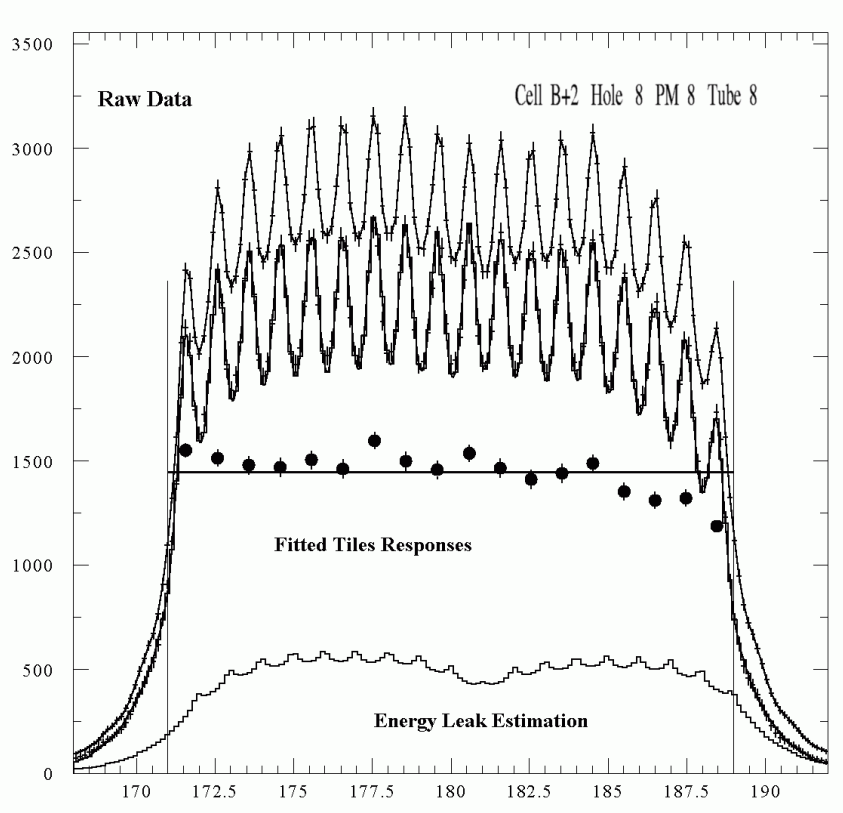


- Minimum Bias current monitoring system
  - It integrates energy to monitor the cell response evolution

# The Monitoring Systems

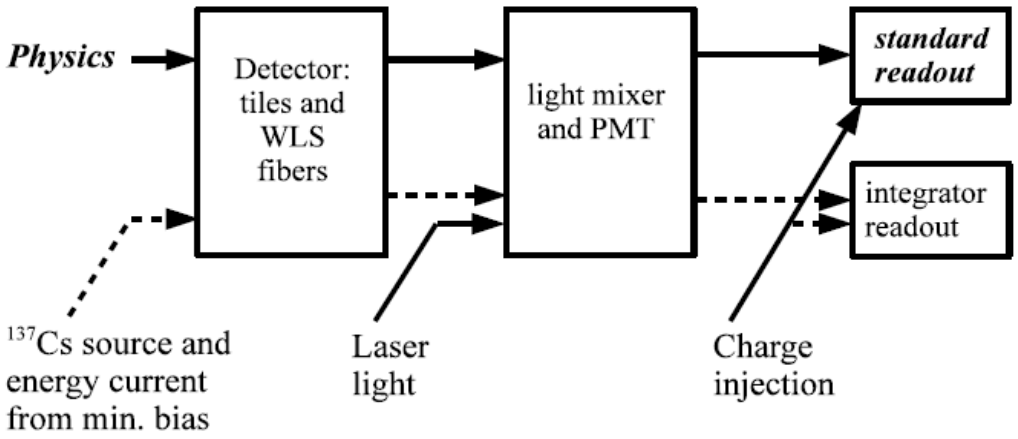


- Charge Injection (stability: 0.7%)
  - The charge produced by the PMT's is digitized by ADC's. The charge injection system using charges stored in capacitors gives correspondence ADC counts->pC and electronics linearity.

# Electromagnetic scale (EM)

- The next step is to relate the pC measured by the PMTs to some "physics" scale to compare experimental and simulated results. This was done by exposing a fraction of the detector modules to electron at TB's
- In ATLAS the HV is set in a way that PMT response to Cs is equal to the one when the EM scale was measured at TB taking into account the Cs lifetime

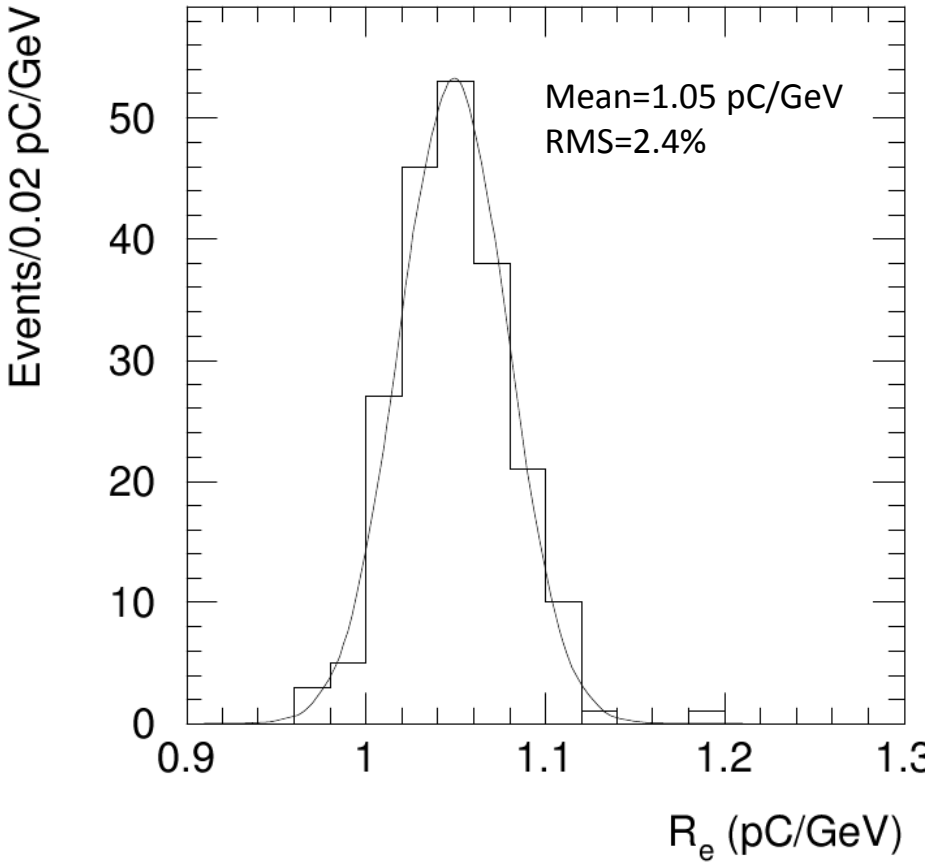

# Energy reconstructed for each channel

$$E = A_{ADC} \times C_{Las} \times C_{Cs} \times C_{\mu/Sr} \times C_{CIS} \times EM$$

- $A_{ADC}$ : Amplitude in ADC
- $C_{Las}$ : Relative variation from Laser system
- $C_{Cs}$ : Relative variation from Cs system
- $C_{\mu/Sr}$ : Factor due to the different sizes of the cells
- $C_{CIS}$ : ADC→pC convertion factor
- EM : pC→GeV conversion factor from *e's* at TB

→ The same energy deposit leads to the same signal at the E.M. scale anywhere in the detector

# Cell Response Variation

- Corrections applied to the PMT response
- Down drift due to high instantaneous luminosity
- Up drift due to recovery during technical stops
- Radiation effects on the scintillating tiles: 2%

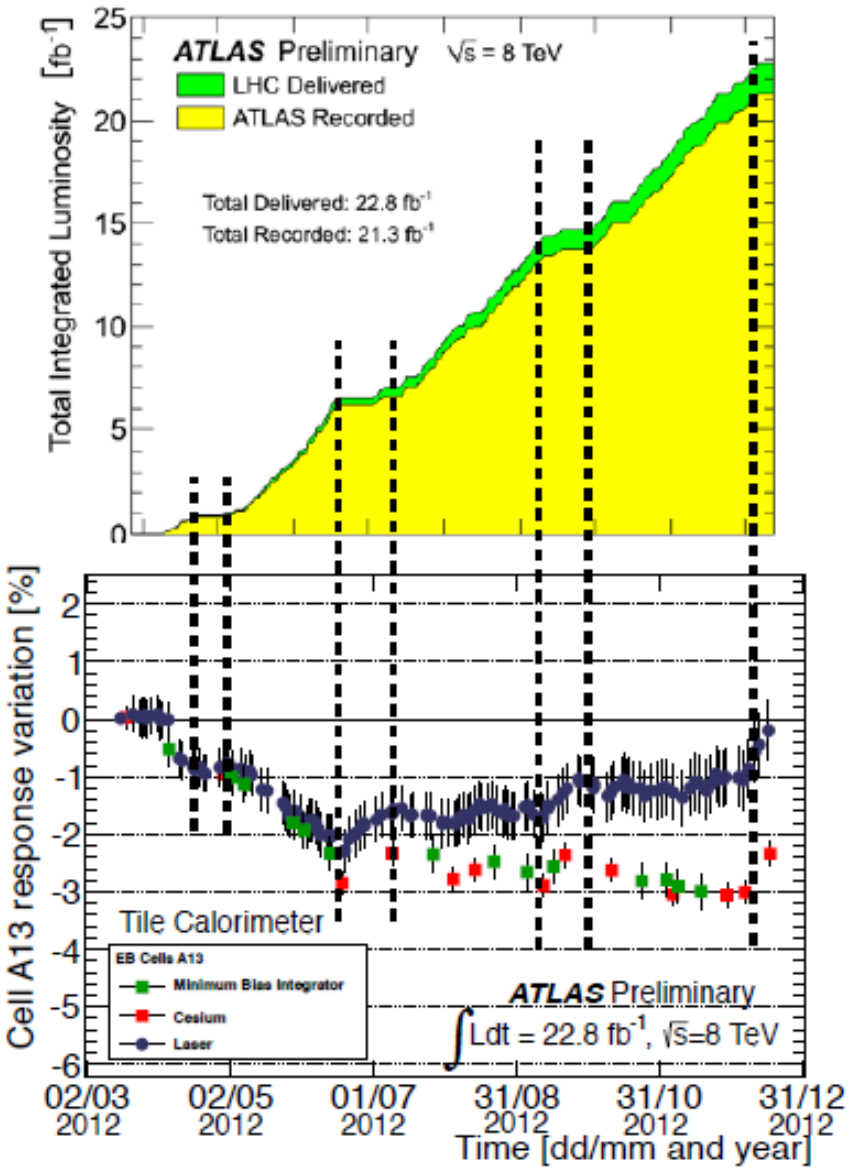

# Performance with single muons

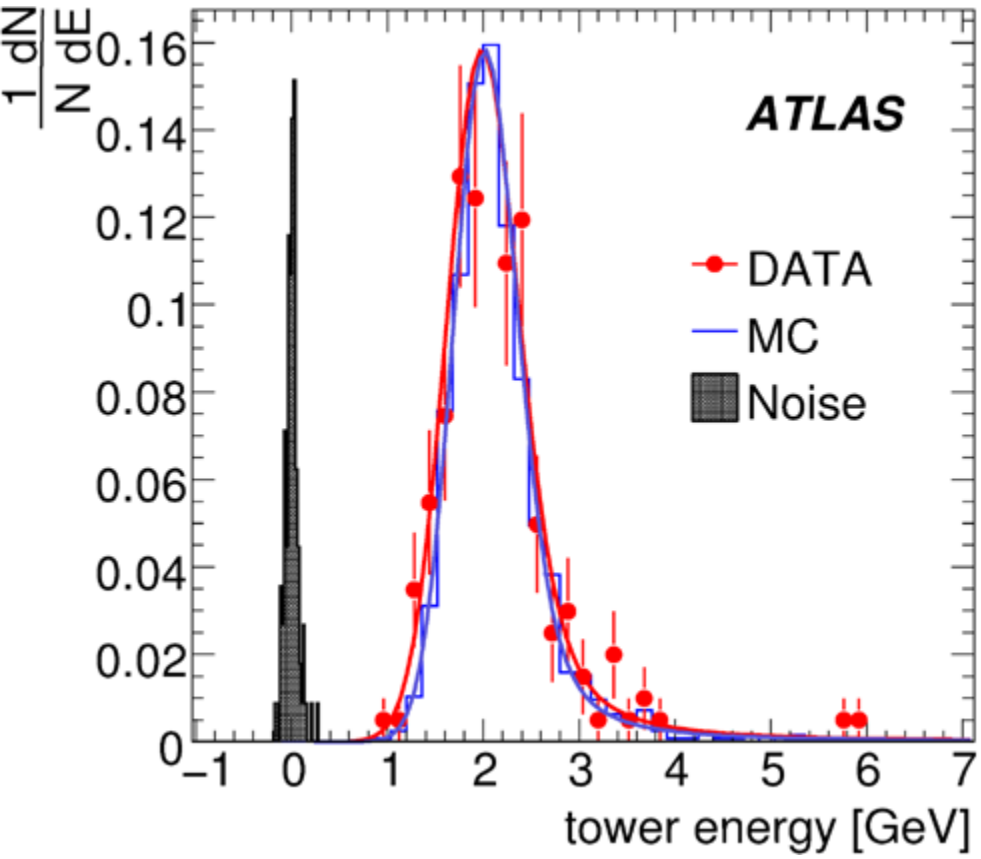


- Muon signal in TileCal is well separated from noise
- Cosmic muons can be used to cross-check cell energy inter-calibration and overall EM scale
- Data and MC dE/dx comparisons as a function of $\eta$ and $\phi$ show good cell inter-calibration within one radial layer (2%)
- Stability in the last 3 years: ≤ 1.5%

# Validation of the EM Scale Using Muons

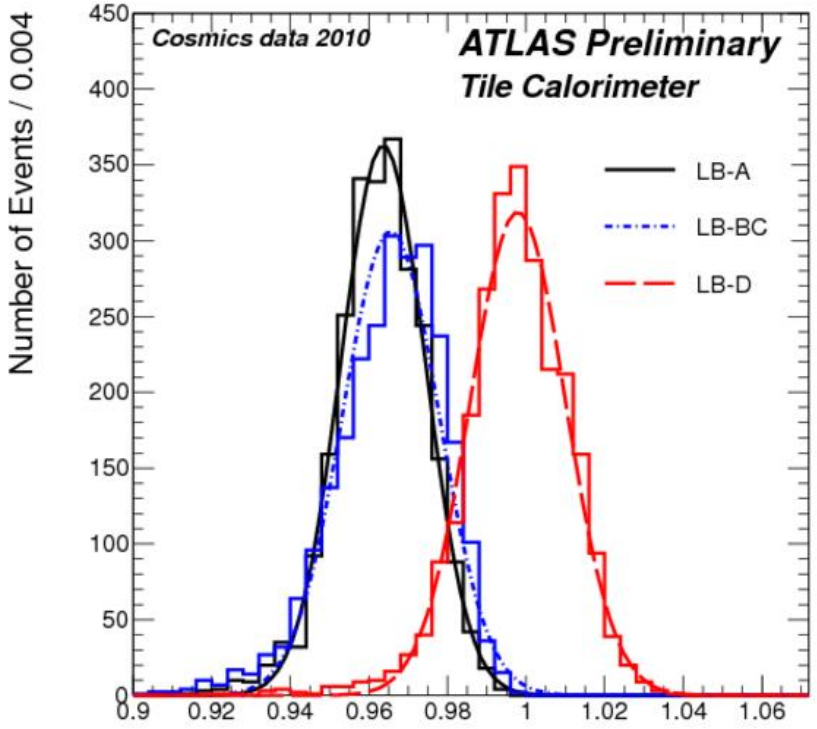


$$R = \left\langle \frac{dE}{dx} \right\rangle_{data} \Big/ \left\langle \frac{dE}{dx} \right\rangle_{MC}$$

- The ratio $R$ allows to compare the actual value of the EM energy scale in ATLAS and the value set at CTB
- The distributions include systematic effects (strongly correlated)
- Difference between barrel layer D and all other layers is observed (4%)

# Jets Measurements

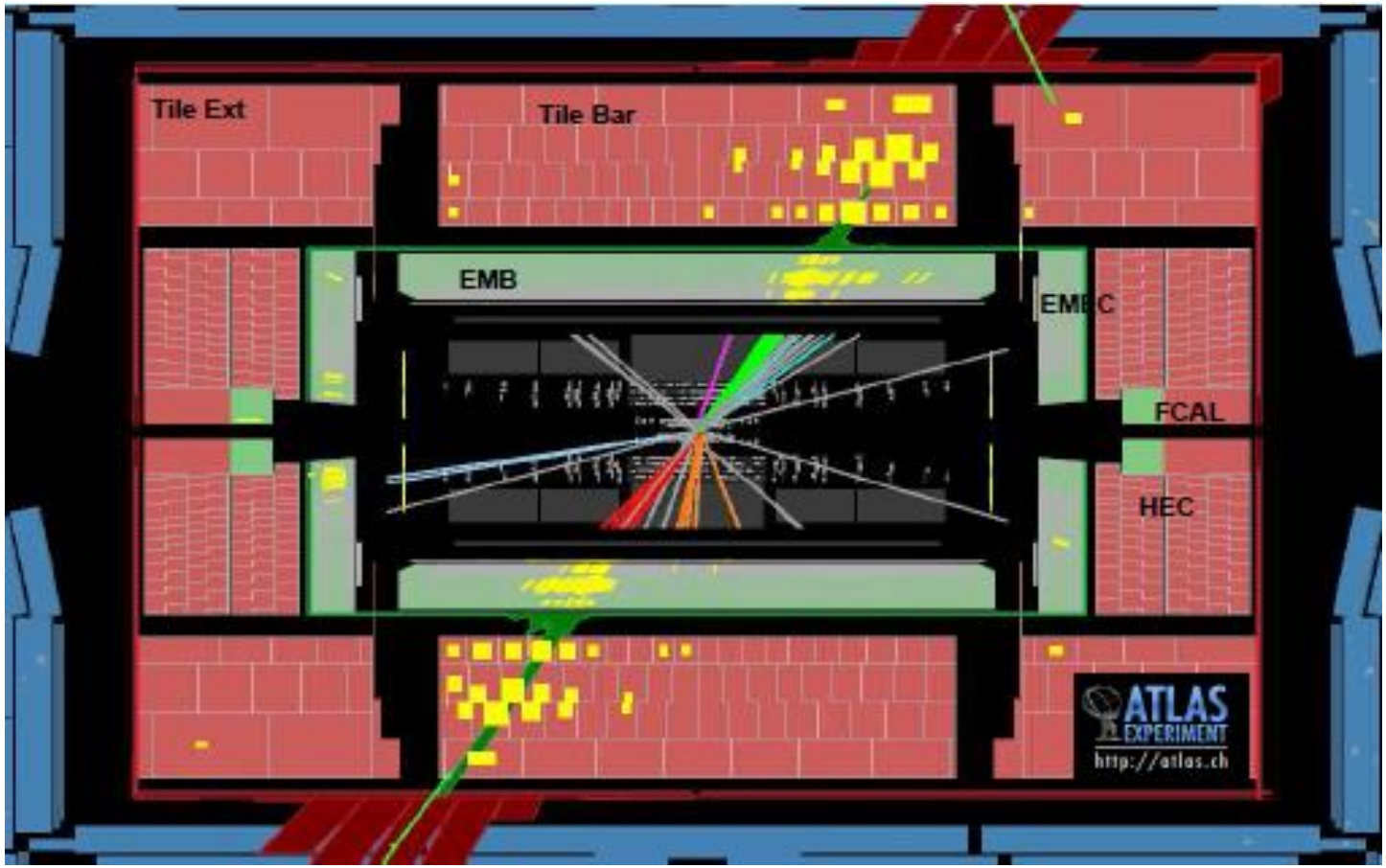


Hadronic calorimeters (depth at $\eta = 0$: 1.2 $\lambda$ + 7.4 $\lambda$) are primarily used to measure the energies of jets:

$$E^{jet} = E^{jet}_{EMC} + E^{jet}_{HADC}$$

→Jet energy linearity, Jet energy resolution, Missing transverse energy resolution

# Jet Energy Calibration

- The jet energy calibration relates the jet energy measured with the ATLAS calorimeter to the energy of the corresponding jet of stable particles entering the ATLAS detector

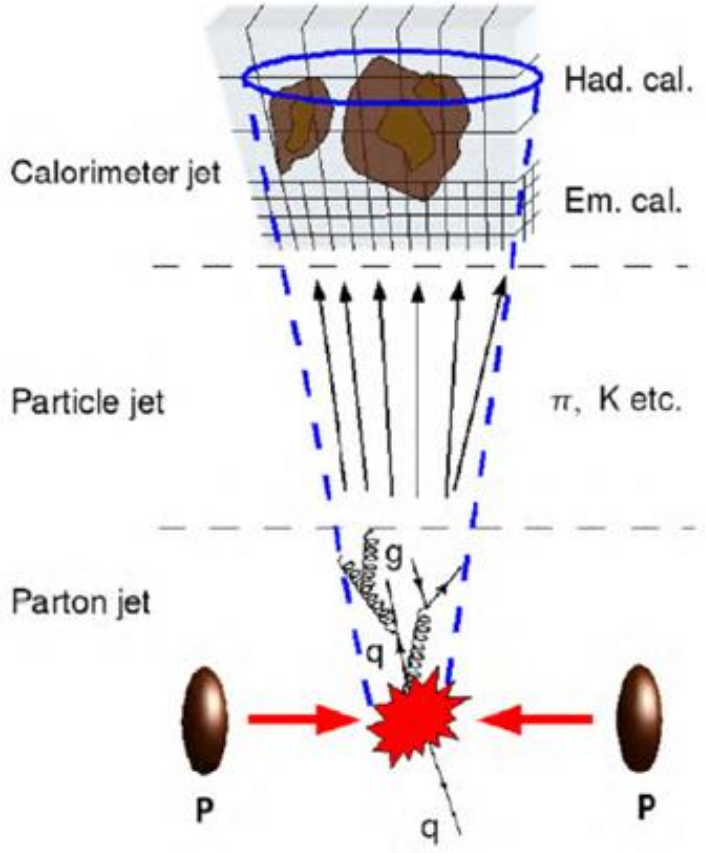

# Topological Calorimeter Clusters

- The energy of jets is estimated by adding the energy deposited in the cell of a cone with half angle $\Delta R = \sqrt{(\Delta\eta)^2 + (\Delta\phi)^2}$ in pseudo-rapidity, $\eta$, and azimuth angle $\phi$ space and whose axis is centered on a seed cell above a pre-defined threshold.
- Jets reconstructed are formed from calorimeters energy depositions reconstructed at the EM scale

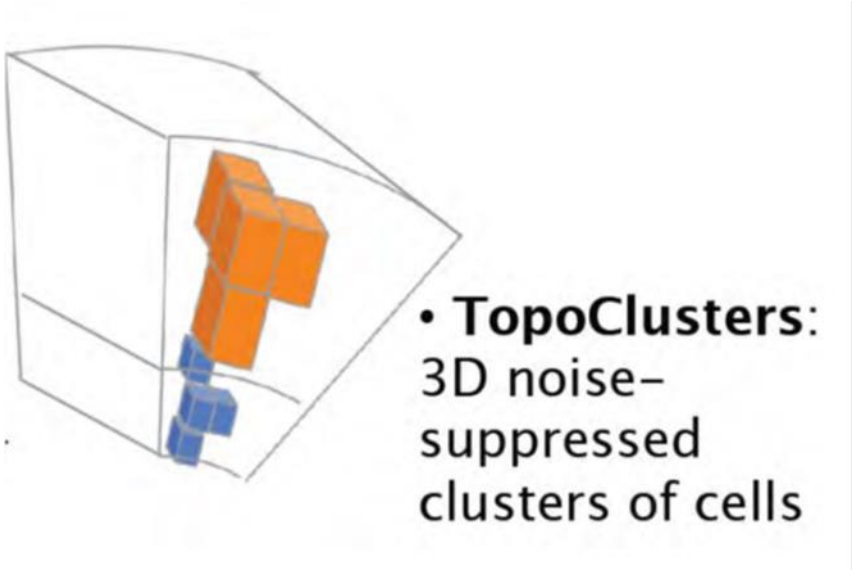

# EM+JES Calibration Scheme

$$E_{calib}^{jet} = \frac{E_{meas}^{jet}}{F_{calib}\left(E_{meas}^{jet}\right)}$$

with $E_{meas}^{jet} = E_{EM}^{jet} - O(N_{PV})$

- $E_{EM}^{jet}$ is measured at the EM scale
- $O(N_{PV})$ is the pile-up offset
- $F_{calib}\left(E_{meas}^{jet}\right)$ is evaluated in η bins using MC jets

# Average JES corrections

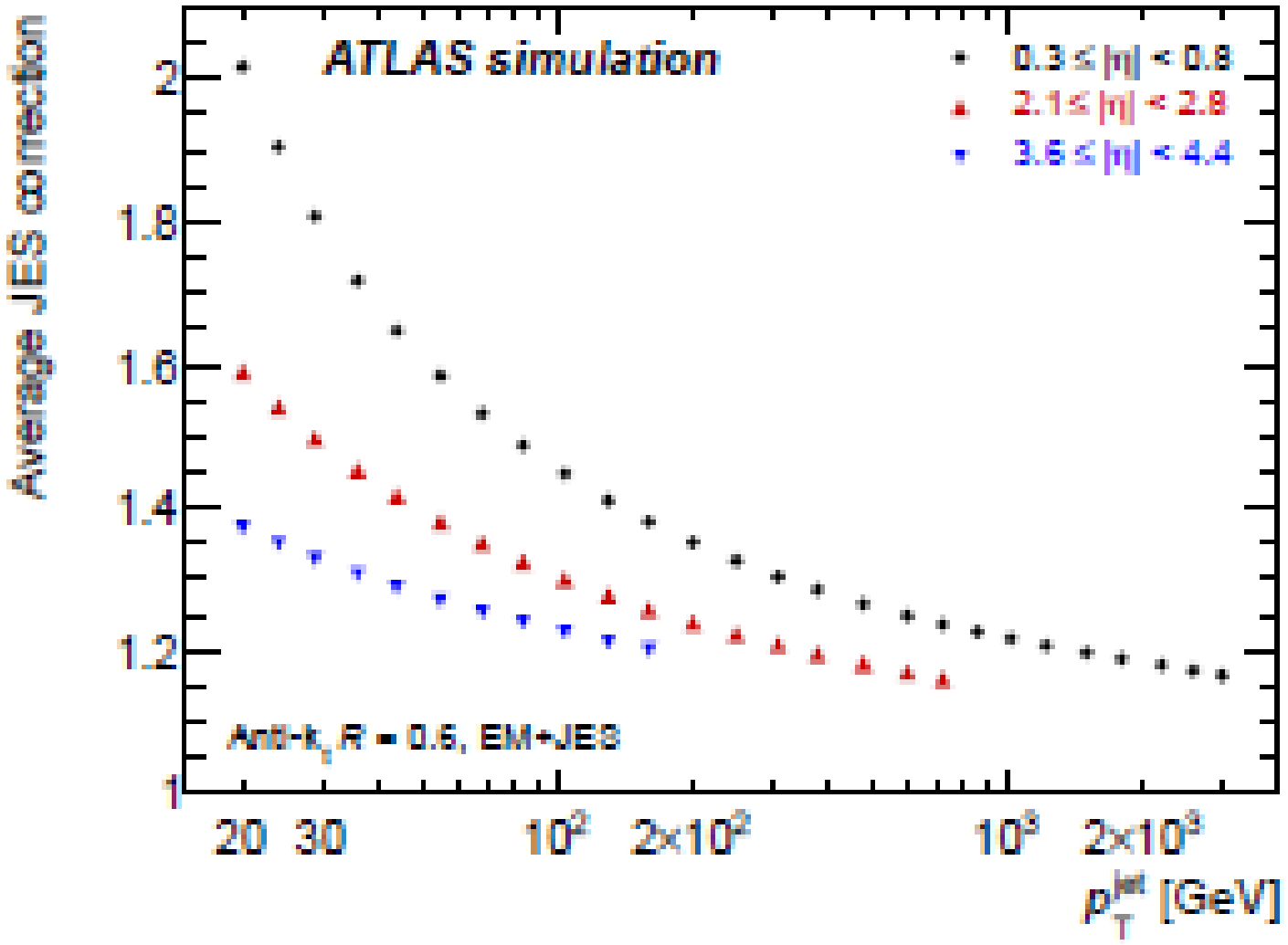

# Uncertainty on the calorimeter response

The uncertainty in the calorimeter response was obtained from the response uncertainty in the individual particles constituting the jet

The following single particle response measurements were used

- In situ single hadron energy measured in a cone around an isolated track with $0.5 \leq p \leq 20$ GeV/c
- The pion response measurements measured in the 2004 CTB where a full slice of the ATLAS detector was exposed to pion beams with momenta between 20 GeV/c and 350 GeV/c

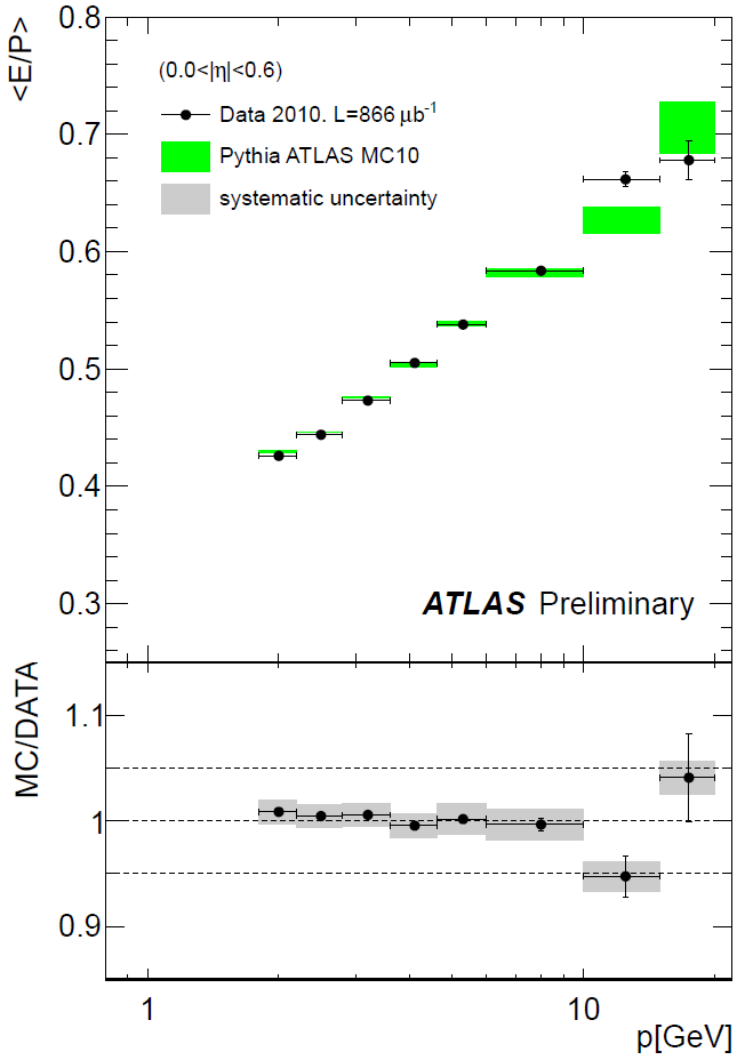

# CTB: Resolution of high energy pions

- The error on the resolution is equal to ≅ 1% for all the energies.
- The energy resolution in general is narrower in the simulation than in the data.

Energy resolution. Data: open points and MC: full points vs. E at η = 0.55

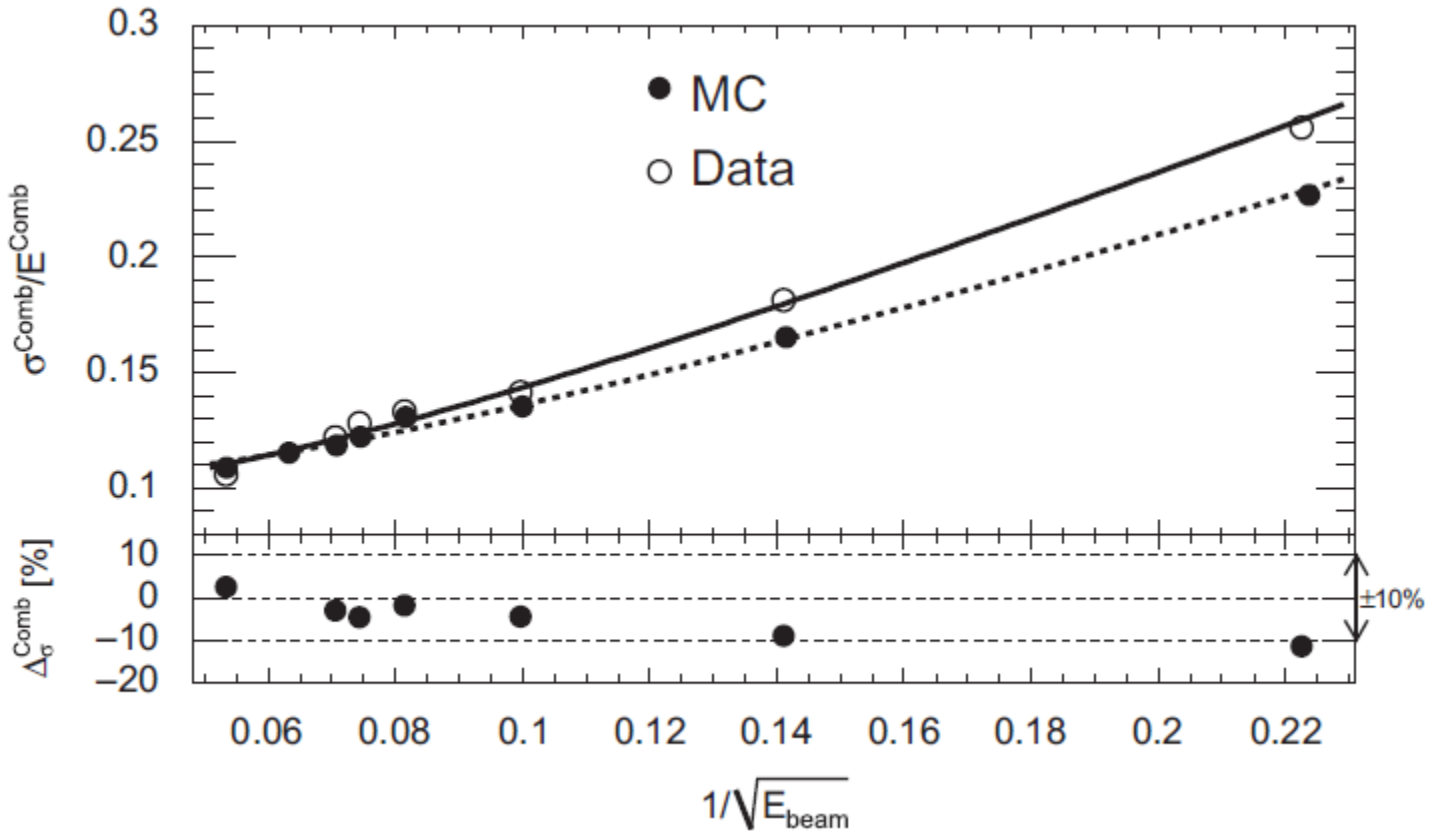

# CTB: Linearity of high energy pions

- The response has been determined with un uncertainty of about 2.5%.
- The MC is able to reproduce the response to within a few percent.

Energy response ratio. Data: open points and MC: full points vs. E at η = 0.35

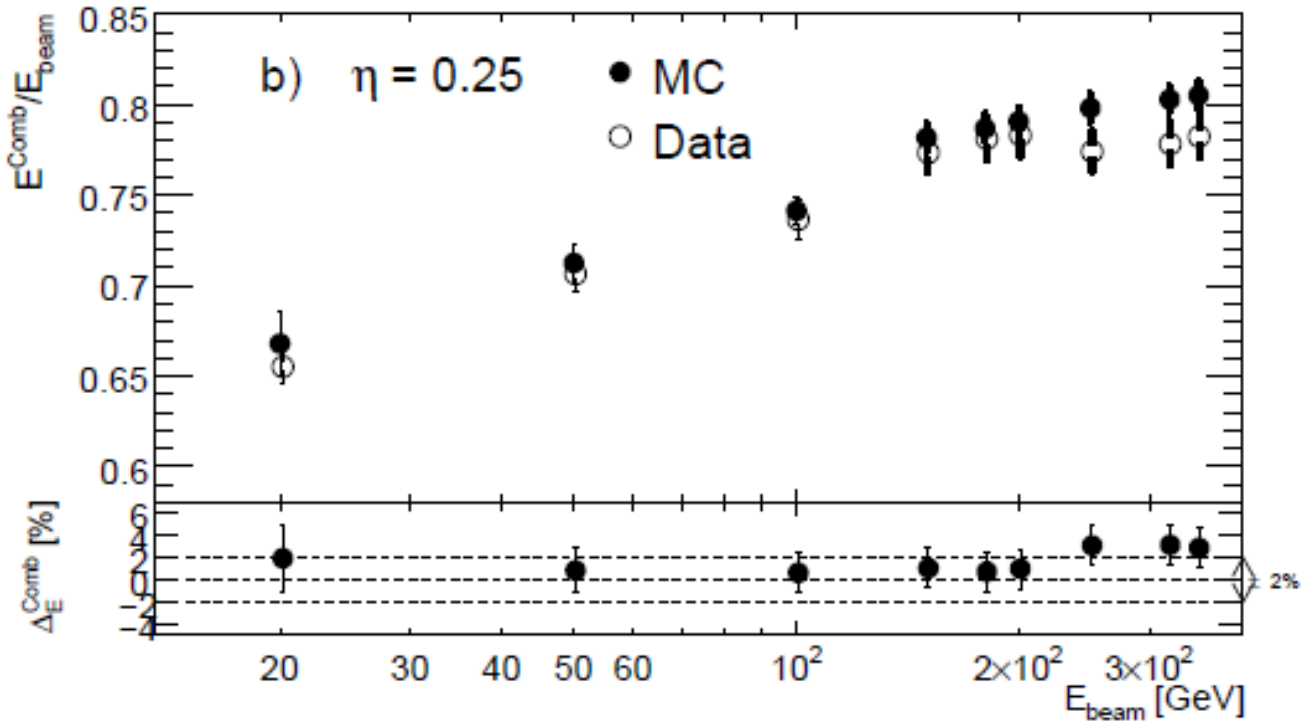

# The EM+JES systematic uncertainty

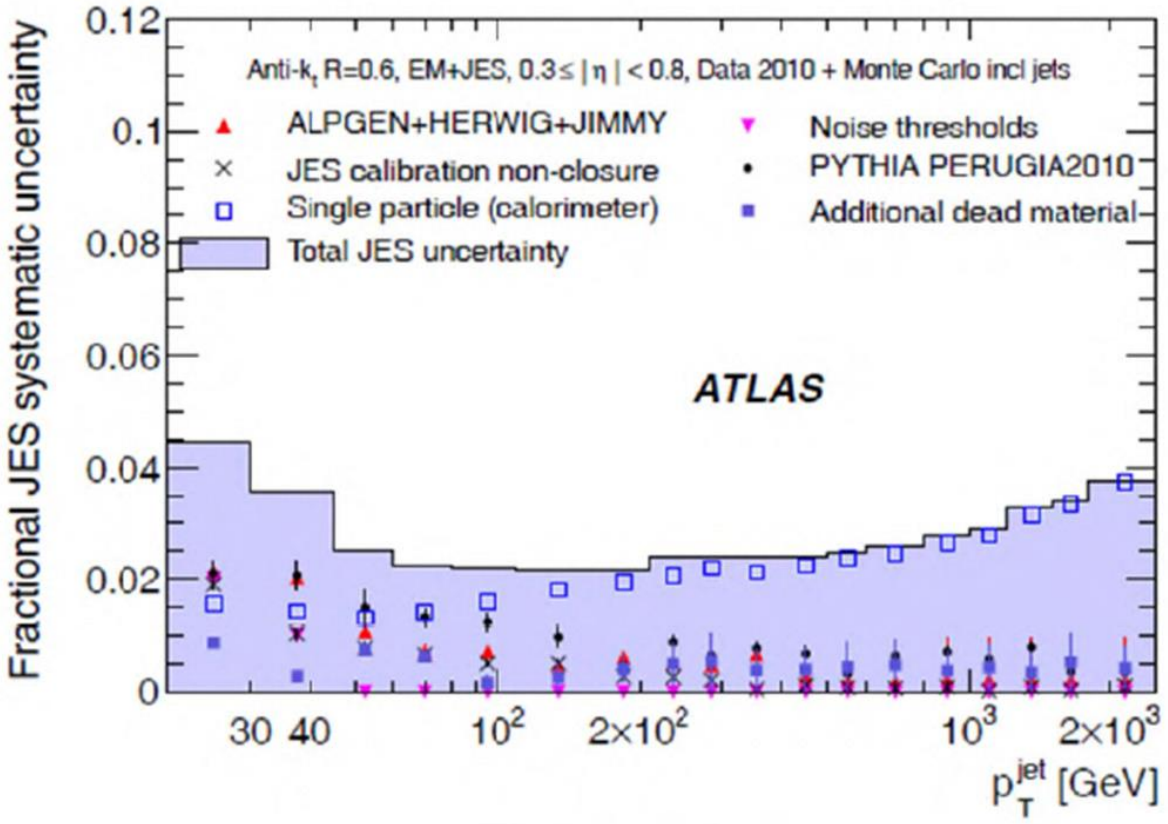


(a) $0.3 \leq |\eta| < 0.8$

# The EM+JES Jet Energy Resolution

The jet energy resolution is determined by exploiting the transverse momentum balance in events containing jets with large transverse momenta

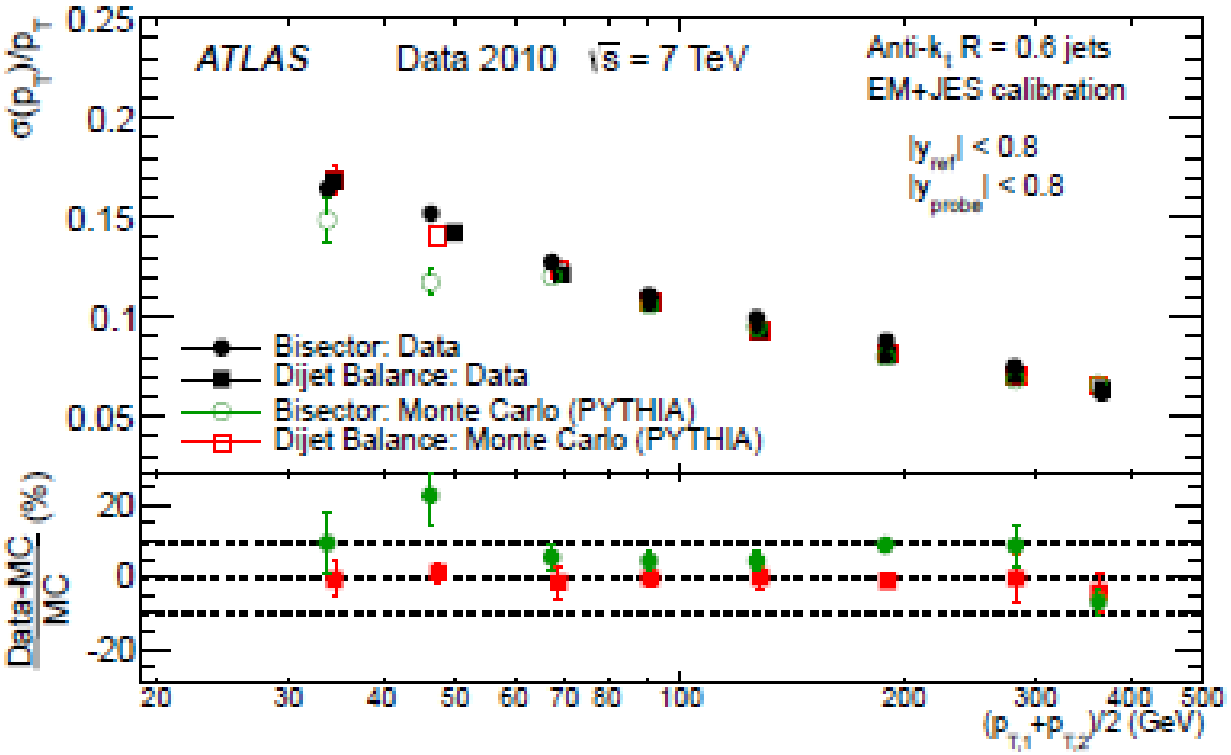

# Beyond the simplistic EM+JES

- The EM+JES calibration facilitates the evaluation of systematic, but the energy resolution is rather poor
  - The contribution of the JES systematic uncertainty on the determination of the $m_{top}$ is 0.79 GeV (The total systematic error is 1.35 GeV)

- More sophisticated calibration schemes will be used in Run 2
  - Global calorimeter cell energy density calibration (GCW)
  - Local cluster calibration (LCW)